Authors

Zachary C. Poss, Christopher C. Ebmeier, Aaron T. Odell, Anupong Tangpeerachaikul, Thomas Lee, Henry E. Pelish, Matthew D. Shair, Robin D. Dowell, William M. Old, and Dylan J. Taatjes

Identification of Mediator Kinase Substrates in Human Cells using Cortistatin A and Quantitative Phosphoproteomics

Graphical Abstract

Authors

Zachary C. Poss, Christopher C. Ebmeier, Aaron T. Odell, ..., Robin D. Dowell, William M. Old, Dylan J. Taatjes

Correspondence

taatjes@colorado.edu

In Brief

Taking advantage of a recently characterized Mediator kinase (CDK8 and CDK19) inhibitor, Poss et al. use SILAC-based proteomics and phosphoproteomics, RNA-seq, and biochemical assays to provide an extensive analysis of human Mediator kinase function. The methods applied and targets identified provide a valuable resource for future studies.

Highlights

- Large-scale identification of CDK8 and CDK19 substrates in human cells

- Seventy-eight high-confidence targets identified within 64 different proteins

- Quantitative proteomics largely show no increased turnover of CDK8/19 targets

- Data support CDK8/19 roles in metabolism and DNA repair, as well as transcription

Accession Numbers

GSE65161
GSE78506

CellPress

Identification of Mediator Kinase Substrates in Human Cells using Cortistatin A and Quantitative Phosphoproteomics

Zachary C. Poss,[1] Christopher C. Ebmeier,[2] Aaron T. Odell,[2,3] Anupong Tangpeerachaikul,[4] Thomas Lee,[1] Henry E. Pelish,[4] Matthew D. Shair,[4] Robin D. Dowell,[2,3] William M. Old,[2] and Dylan J. Taatjes[1,*]

[1]Department of Chemistry and Biochemistry, University of Colorado, Boulder, CO 80303, USA
[2]Department of Molecular, Cell, and Developmental Biology, University of Colorado, Boulder, CO 80309, USA
[3]BioFrontiers Institute, University of Colorado, Boulder, CO 80309, USA
[4]Department of Chemistry and Chemical Biology, Harvard University, Cambridge, MA 02138, USA
*Correspondence: taatjes@colorado.edu
http://dx.doi.org/10.1016/j.celrep.2016.03.030

SUMMARY

Cortistatin A (CA) is a highly selective inhibitor of the Mediator kinases CDK8 and CDK19. Using CA, we now report a large-scale identification of Mediator kinase substrates in human cells (HCT116). We identified over 16,000 quantified phosphosites including 78 high-confidence Mediator kinase targets within 64 proteins, including DNA-binding transcription factors and proteins associated with chromatin, DNA repair, and RNA polymerase II. Although RNA-seq data correlated with Mediator kinase targets, the effects of CA on gene expression were limited and distinct from CDK8 or CDK19 knockdown. Quantitative proteome analyses, tracking around 7,000 proteins across six time points (0–24 hr), revealed that CA selectively affected pathways implicated in inflammation, growth, and metabolic regulation. Contrary to expectations, increased turnover of Mediator kinase targets was not generally observed. Collectively, these data support Mediator kinases as regulators of chromatin and RNA polymerase II activity and suggest their roles extend beyond transcription to metabolism and DNA repair.

INTRODUCTION

An important first step in understanding the cellular function of kinases is to identify the substrates that they modify. This first step has remained a persistent challenge, in part because of the difficulties in the development of highly potent and selective kinase inhibitors. The human CDK8 kinase exists in a 600-kDa complex known as the CDK8 module, which consists of four proteins (CDK8, CCNC, MED12, and MED13). The CDK8 module associates with regulatory loci on a genome-wide scale (Kagey et al., 2010; Pelish et al., 2015), and global targeting of the CDK8 module appears to reflect its association with Mediator (Allen and Taatjes, 2015). CDK19, a paralog of CDK8, emerged

in vertebrates and has high sequence similarity to CDK8, including nearly identical cyclin binding and kinase domains. Comparatively little is known about CDK19; however, it appears to assemble into an analogous CDK19 module in human cells (Daniels et al., 2013).

Based upon their association with Mediator—a global regulator of RNA polymerase II (pol II) transcription—CDK8 or CDK19 may broadly impact gene expression patterns; however, physical knockdown of CDK8 or CDK19 protein levels had relatively modest effects in HCT116 cells, with 2-fold or greater changes in expression of several hundred genes (Donner et al., 2010; Galbraith et al., 2013). Whereas knockdown studies do not address the role of the kinase activity per se, these data suggested limited roles for the Mediator kinases in transcriptional regulation. In agreement, gene expression analyses with the CDK8 ortholog in yeast, Srb10 (Holstege et al., 1998), revealed that about 3% of genes were regulated by Srb10 kinase activity. Similarly, limited effects on yeast transcription were observed in vitro and in vivo upon selective inhibition of Srb10 (CDK8) kinase activity using an analog-sensitive mutant (Liu et al., 2004). Most genes affected by kinase-inactive mutant Srb10 (CDK8) were involved in cellular response to nutrient stress (Holstege et al., 1998).

The biological roles of human CDK8 and CDK19 remain poorly understood, in part because a more-comprehensive identification of their substrates or the genes specifically regulated by their activities has been lacking. Our recent studies with the natural product, cortistatin A (CA), showed that CA is a potent and highly selective inhibitor of the Mediator kinases CDK8 and CDK19 (Pelish et al., 2015). CA binds the CDK8-CCNC dimer with sub-nanomolar affinity (Kd = 195 pM) and two distinct kinome profiling assays, which collectively probed approximately 400 kinases, ultimately confirmed only CDK8 and CDK19 as targets of CA, even with analyses completed at 100 times the measured half-maximum inhibitory concentration (IC_{50}) for CDK8 (Pelish et al., 2015). Given these and other data showing the unusual selectivity of CA, we could begin to probe the cellular function and targets of CDK8 and CDK19.

Here, we report the large-scale identification of Mediator kinase (CDK8 and CDK19) substrates in human cells, using stable

isotope labeling of amino acids in cell culture (SILAC)-based phosphoproteomics. We couple these results with global analysis of gene expression changes (RNA sequencing [RNA-seq]) that result from targeted inhibition of Mediator kinase activity. Furthermore, we assess potential Mediator kinase effects on protein turnover using quantitative proteomic analyses across six time points spanning 24 hr of Mediator kinase inhibition. HCT116 cells were chosen for this study for several reasons. First, although CA potently inhibits Mediator kinase activity in HCT116 cells (Pelish et al., 2015), proliferation is not affected. This eliminated potential confounding effects, such as induction of cell-cycle arrest or death, which could have complicated our analyses. Second, CDK8 is a colon cancer oncogene that was uncovered, in part, by a small hairpin RNA (shRNA) screen in HCT116 cells (Firestein et al., 2008). Third, published gene expression data exist in HCT116 cells with stable CDK8 or CDK19 knockdown (Donner et al., 2010; Galbraith et al., 2013), which allowed us to directly compare and de-couple the effects of subunit knockdown versus targeted inhibition of kinase activity.

RESULTS

Quantitative Phosphoproteomics in HCT116 Cells ± CA

To identify cellular CDK8 and CDK19 substrates, we used SILAC coupled with a phosphoproteomics workflow. Experiments were completed in HCT116 cells supplemented with heavy (Arg10 and Lys8) or light (Arg0 and Lys0) amino acids. Control (DMSO) and CA-treated cells were harvested and mixed 1:1 based on total protein content (CA structure shown in Figure 1A). Phosphopeptides were isolated using titanium enrichment, followed by offline electrostatic repulsion hydrophilic interaction chromatography (ERLIC) with liquid chromatography-tandem mass spectrometry (LC-MS/MS) for phosphosite identification (Figure 1B). We collected 24 fractions during ERLIC fractionation, with an average phosphopeptide enrichment of over 50% in biological triplicate experiments (Figure 1C). In total, over 16,000 heavy-light (H/L) phosphosite ratios were quantified (Table S1) and over 12,000 were present in at least two biological replicates (Figure 1D).

The majority of phosphosites were unaffected by CA treatment, clustering around zero in a $\log_2$ plot of H/L SILAC ratios across replicate experiments (Figure 1D). This result indicated good reproducibility and provided further validation of CA specificity. Many decreased phosphosites were highly correlated across replicates (highlighted green in Figure 1D); in addition, we identified a smaller number of phosphosites that increased upon CA treatment (highlighted peach in Figure 1D; Table S2). Representative mass spectra for SILAC pairs shown in Figures 1E and 1F are from experiments in which either light (E) or heavy (F) cells were treated with CA. For two of three replicates, the heavy population of cells was CA treated, whereas in one replicate, light cells were CA treated, representing a label swap. For data analysis purposes, a reciprocal of the H/L ratio was calculated for the label swap experiment, such that decreased H/L ratios could be evaluated across all biological replicates.

Mediator Kinase Substrates Are Largely Transcription-Associated Proteins

The phosphoproteomics workflow in Figure 1B identified novel phosphosites whose intensities decreased significantly with CA treatment (Figure 2A). We identified 78 phosphosites, represented in 64 proteins, that we designated as high confidence based upon (1) their quantification in at least two of three biological replicates, (2) a reproducible mean H/L ratio across replicates, and (3) a significant decrease in H/L ratio with CA treatment as determined by an empirical Bayes analysis (Margolin et al., 2009; Ritchie et al., 2015). These high-confidence phosphosites are summarized in Table 1 and Figure 2A, and all quantified phosphosites are shown in Table S1. To ensure that a reduced H/L ratio did not result simply from a change in protein level, we completed a quantitative proteome analysis in parallel with phosphoproteomics. Importantly, very few high-confidence phosphosites exhibited any change at the protein level with 1 hr of CA treatment (Table S2). Those that did change somewhat were FOXC1, MAML1, KDM3A, and ATF2, although some of these changes were not consistent across deep proteome replicates, and most of the phosphosite changes remained significant even after accounting for small changes in protein level. Although phosphosites not designated as high-confidence sites could represent bona fide Mediator kinase substrates (e.g., those that are quantified in only one biological replicate), we will only discuss targets designated as high confidence based on the criteria above.

To determine whether an H/L ratio for a phosphosite changed significantly with CA treatment across replicates, we employed an empirical Bayes statistical approach using the *limma* software package (Ritchie et al., 2015). An empirical Bayesian framework allowed for the calculation of adjusted p values for each phosphosite (Figure 2B). This approach can account for experiment-specific differences, which is advantageous compared to more arbitrary approaches, such as a universal fold-change cutoff (Margolin et al., 2009). We found that more phosphosite ratios decreased than increased upon CA treatment, as expected with targeted kinase inhibition for a short amount of time. This is shown by a higher number of data points on the left side of the volcano plot compared to the right side, using an adjusted p value cutoff of 0.1 (Figure 2B; see also the Supplemental Note in Supplemental Information).

We used iceLOGO (Colaert et al., 2009) to determine statistically enriched motifs within the identified Mediator kinase substrates. We found that the majority of the phosphosites contained an S/T-P motif (Figure S1A). Additionally, a proline at the −2 and −1 positions relative to the phosphorylation site was over-represented. These data support the notion that many CDK8 phosphorylation sites occur within PX(S/T)P motifs as previously suggested (Alarcón et al., 2009; Bancerek et al., 2013). Serine was more frequently phosphorylated than threonine (Figure S1A), and we did not see evidence for over-representation of basic residues at positions C-terminal to the phosphosite, as observed with other CDK motifs (Ubersax and Ferrell, 2007).

Because few substrates for human CDK8/19 have been identified, the analysis uncovered many phosphosite targets (Table 1). Many targets are DNA-binding transcription factors (TFs), chromatin regulators, or other known regulators of pol II activity
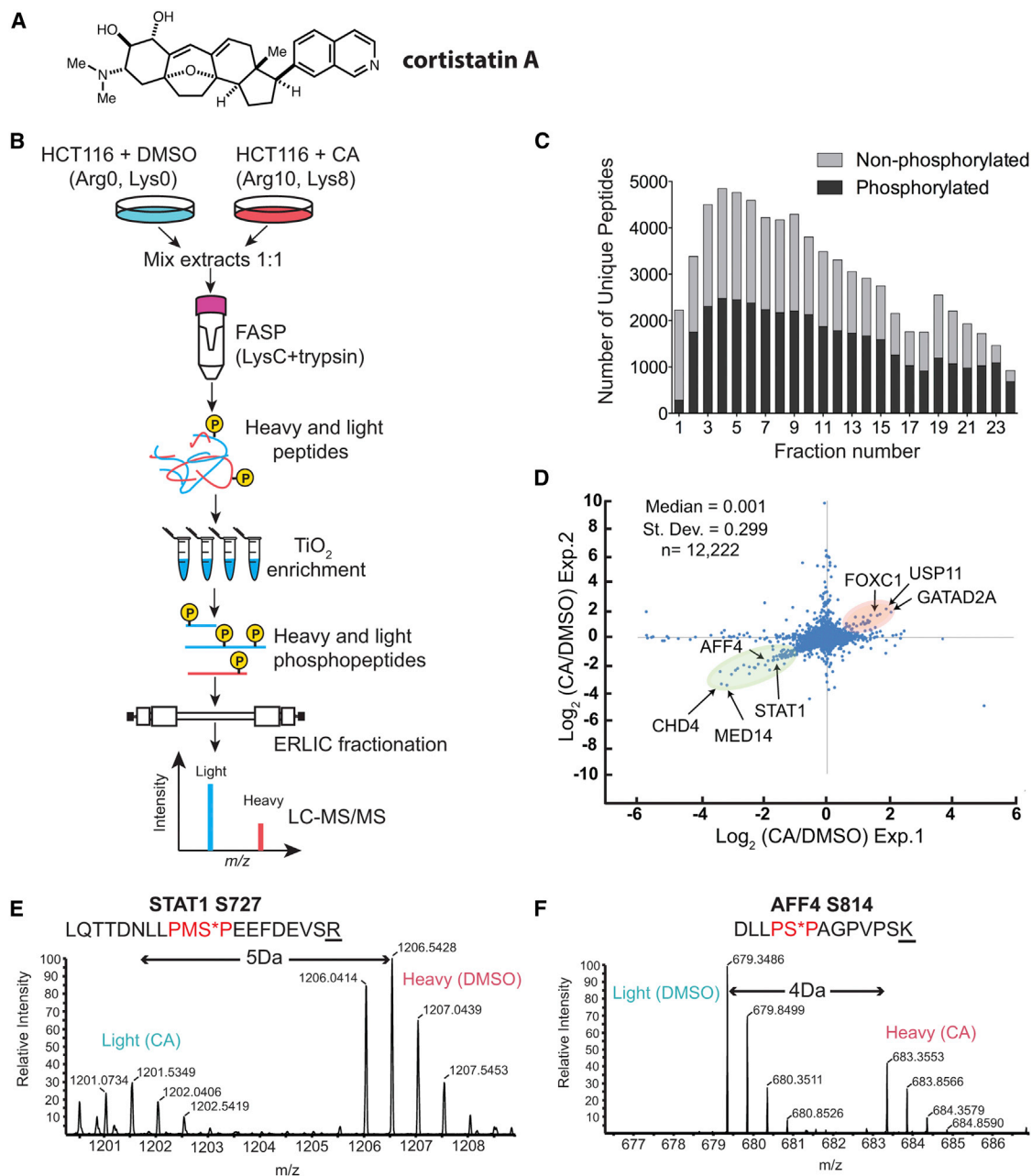
Figure 1. Quantitative Phosphoproteomics in HCT116 Cells ± CA

(A) Cortistatin A (CA) structure.

(B) Overview of phosphoproteomics workflow used to identify Mediator kinase substrates.

(C) Unique phosphopeptides identified with LC-MS/MS after ERLIC fractionation. Average of biological triplicates is represented.

(D) CA treatment with quantitative phosphoproteomics reproducibly identifies Mediator kinase substrates. H/L ratios quantified in two of three biological replicates are plotted on the x and y axes. Plot shows proteins whose H/L ratios decrease (green) and increase (peach) upon CA treatment.

(E and F) Representative mass spectra. Spectra shown are from replicates in which either the light (E) or heavy (F) cells were CA treated. Differences in SILAC pairs are shown based on the labeled amino acid; Arg(10) in (E) and Lys(8) in (F). The charge is +2 for both peptides.

(Figures 2A and S1B), consistent with the established role of CDK8 in transcription. Additional substrates, including proteins implicated in DNA replication and repair (BRCA1 and MDC1) and ubiquitination (HUWE1 and CUL4B) suggest biological roles for Mediator kinases beyond transcription. A known

CDK8 substrate, STAT1 S727 (Bancerek et al., 2013), was identified as a high-confidence target, and other novel phosphosites reside in proteins that interact with CDK8-Mediator and/or the CDK8 module, including AFF4, MAML1, and Mediator subunits (Figure 2A; Table 1). AFF4 is a core component of the
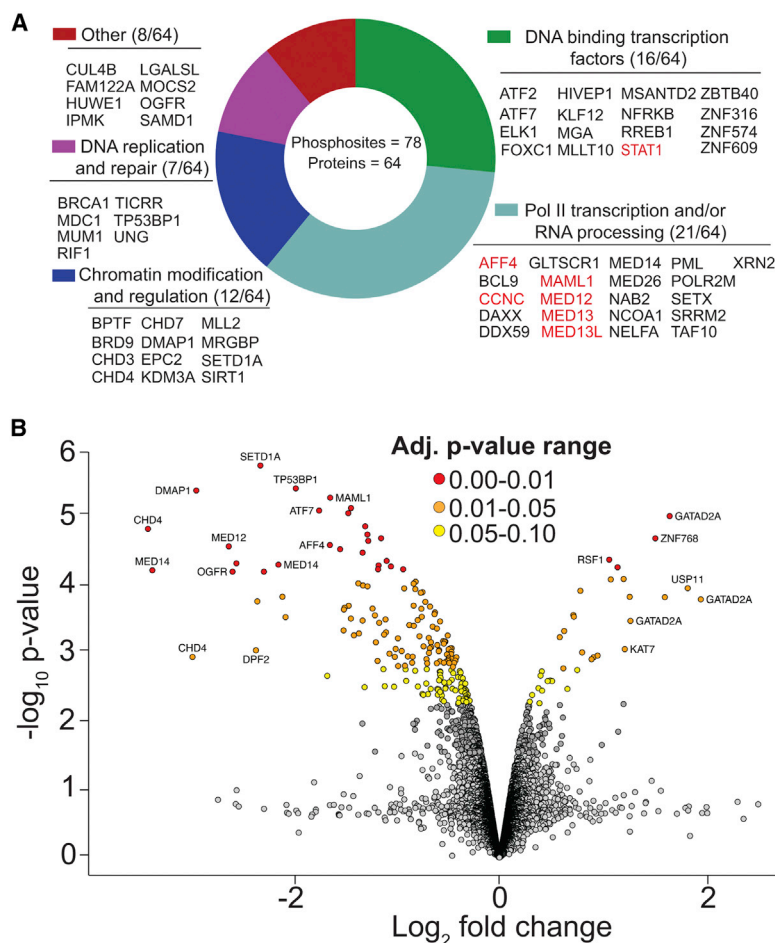
Figure 2. Identification of Mediator Kinase Substrates

(A) Functional categorization of high-confidence Mediator kinase substrates identified.

(B) Volcano plot of statistically significant phosphosite changes with CA treatment using an empirical Bayes analysis.

assays, western blots, and MS experiments. We selected proteins representing different classes of substrates (Figure 2A) for further evaluation. The DNA-binding TF STAT1, a previously identified CDK8 kinase substrate (Bancerek et al., 2013), was probed by western blot in interferon (IFN)-γ-induced HCT116 cells (Figure 3A). This experiment confirmed STAT1 S727 as a Mediator kinase substrate in HCT116 cells and also showed CA-dependent inhibition at low nM concentrations, as reported previously (Pelish et al., 2015).

Among the chromatin modification and regulation substrates, we examined SIRT1, in part because an antibody against the phosphorylated SIRT1 T530 site was commercially available. When HCT116 cells were treated with CA, we noted a decrease in SIRT1 T530 phosphorylation (Figures 3B and 3C). Total SIRT1 levels were unaffected by CA treatment, and levels of the CDK8 module subunits CDK8, CCNC, and MED12 were not changed by treatment with the compound (Figure 3B). The approximately 50% reduction in phospho-SIRT1 did not change with increasing CA concentration, indicative of CA selectivity (Pelish et al., 2015). Although other kinases, such as CDK1 and JNK, are known to phosphorylate this site (Sasaki et al., 2008), treatment with inhibitors of CDK1 (RO-3306) and JNK family kinases (SP600125) did not seem to impact SIRT1 T530 phosphorylation; in fact, we were unable to completely reduce SIRT1 phospho-T530 detection, even when treating with all three inhibitors (Figure S2). In vitro kinase assays with purified CDK8 module and SIRT1 confirmed CDK8-dependent SIRT1 T530 phosphorylation by western blot (Figure 3D).

Next, we tested two different substrates, RIF1 and TP53BP1, linked to DNA replication and repair. Because these proteins are very large (each over 200 kDa), we expressed glutathione S-transferase (GST)-tagged fragments (ca. 100 residues) surrounding the phosphosite. As shown in Figure 3E, the CDK8 module phosphorylated these substrates, whereas point mutations (S to A) at the identified phosphorylation site(s) greatly reduced substrate phosphorylation, supporting these sites as CDK8 module targets in vitro (Figure 3E).

We also confirmed phosphorylation sites in MED12 and MED13 using in vitro kinase assays using the recombinant

super-elongation complex (SEC) (Luo et al., 2012), which co-purifies with CDK8-Mediator (Ebmeier and Taatjes, 2010), and MAML1 is a Notch pathway co-activator that recruits CDK8 to Notch-dependent genes where it phosphorylates the Notch ICD (Fryer et al., 2004).

We submitted the 64 CDK8/19 substrate proteins to the STRING protein-protein interaction database (Szklarczyk et al., 2015) and found that six Mediator complex subunits, three subunits of the TIP60/NuA4 complex (EPC2, DMAP1, and MRGBP), and two subunits of the NuRD complex (CHD3 and CHD4) were represented (high-confidence score ≥ 0.7; Figure S1C). The TIP60/NuA4 and NuRD complexes are multi-subunit assemblies that possess multiple enzymatic activities, including nucleosome remodeling, acetyltransferase, and deacetylase activities. Additionally, this analysis identified a network of interacting proteins involved in DNA damage repair (Figure S1C), as well as an interaction between XRN2 and SETX. Taken together, these data suggest that Mediator kinases regulate multiple and diverse cellular processes, potentially via several distinct multi-subunit assemblies.

Validation of Selected Mediator Kinase Substrates

To further validate the CDK8/19 substrates identified with SILAC-based phosphoproteomics, we performed in vitro kinase

CDK8 module (containing CDK8, CCNC MED12, and MED13) purified from insect cells. Incubation of the CDK8 module with ATP and subsequent TiO_2 enrichment and MS analysis confirmed both S688 on MED12 and S749 on MED13 as substrates (Figures 3F and 3G). We did not identify the CCNC site from these experiments because the site identified from CA-treated HCT116 cells is not present in the canonical CCNC isoform used for recombinant CDK8 module expression and purification.

The data summarized in Figure 3 verified each of seven high-confidence Mediator kinase sites, representing about 10% of all high-confidence sites listed in Table 1. These results, combined with previous data demonstrating CA potency and specificity (Pelish et al., 2015), support the substrates listed in Table 1 as Mediator kinase targets. Although extensive kinome profiling has demonstrated CA specificity, we conducted in vitro kinase assays using a shared substrate, the pol II CTD, and found that CDK1, ERK2, and GSK3β activity was unaffected by CA treatment, even at concentrations 10-fold above those used for proteomic and gene expression analyses (Figure 3H).

Mediator Kinase Inhibition Has Limited and Specialized Effects on Transcription

As Mediator-associated kinases, it was plausible that inhibition of CDK8 and CDK19 activity could affect expression of large numbers of genes. We analyzed gene expression (RNA-seq) data from CA-treated HCT116 cells (Table S3). To minimize secondary or indirect effects resulting from long-term Mediator kinase inhibition, we completed RNA-seq after a 3-hr CA treatment (100 nM); this also helped match mRNA changes with measured phosphorylation changes that were determined after 1-hr CA treatment. RNA-seq analysis identified 150 genes whose expression changed significantly with CA treatment (Figure 4A). Among these genes, the magnitude of change in expression was modest (largely 1.2- to 2-fold), indicating that CDK8/19 activity per se is not a major driver of their transcription, at least in the context of this analysis (HCT116 cells under normal growth conditions). Such modest gene expression changes were also observed in CA-sensitive cell lines (e.g., MOLM-14), although the genes affected were distinct (Pelish et al., 2015).

Gene Expression Changes in CA-Treated Cells Compared to CDK8 or CDK19 Knockdown

Because CA inhibits both CDK8 and CDK19 kinases, we used previously published HCT116 microarray datasets (normal growth conditions), in which either CDK8 or CDK19 had been stably knocked down (Donner et al., 2010; Galbraith et al., 2013), as a comparison to CA-treated HCT116 cells. Only genes exhibiting 1.5-fold change in expression or greater, with p values < 0.05, were used from the microarray data; these genes were compared to our RNA-seq analysis in which cells were treated with 100 nM CA for 3 hr. We observed only a modest overlap among genes differentially expressed (Figure 4B; note that because CA inhibits both CDK8 and CDK19, gene sets for CDK8 or CDK19 knockdown were combined). Because cellular knockdown experiments take over 24 hr to manifest, the modest

correlation in gene expression changes could reflect the short time of CA treatment. However, RNA-seq analyses after 24 hr CA treatment revealed similarly low numbers of shared gene expression changes (Figure 4C). These results, further summarized in Figure S3, suggest that the physical presence of the CDK8 or CDK19 protein has distinct effects on transcription compared to targeted kinase inhibition.

Functional Links between Gene Expression Changes and Mediator Kinase Substrates

Because many Mediator kinase substrates are TFs (Figure 2A), we hypothesized that some of the observed differences in gene expression due to CDK8/19 inhibition might be caused by changes in TF function. To begin to address this hypothesis, we extracted promoter sequences (±2 kb from the transcription start site [TSS]) for genes that were differentially expressed (increased or decreased expression) 3 hr CA treatment. F-Match was then used to compare promoter sequences to controls to determine whether any TF-binding sites, reported as Transfac matrices, were over-represented. The ratio of this increase (CA-treated cells versus DMSO controls) is displayed for over-represented sites in Figure 4D. We found that many of the identified Transfac matrices for genes whose expression increased or decreased with CA treatment were mutually exclusive (Figure 4D). That is, an enriched TF-binding site in CA increased genes was generally not present in CA-decreased genes and vice versa. A hypergeometric test confirmed a significant overlap (p value = $1.15E^{-5}$) between Mediator kinase targets identified in Table 1 and Transfac matrices identified in our gene expression promoter analysis (Figure S3F).

Many of the Transfac matrices identified by F-match (Figure 4D) can be traced back to Mediator kinase activity, as summarized in Figure S4. For example, the RREB1 TF was identified in both the F-match analysis (RREB1_01) and the SILAC phosphoproteomics (Table 1). Enriched TF-binding sites were observed for genes with altered expression in CA-treated HCT116 cells (Figure 4A), including MYC, a β-catenin target gene; EGR1 (i.e., KROX_Q6); and HES1, a Notch pathway target gene. Moreover, the MGA and NAB2 proteins, each high-confidence Mediator kinase substrates, are known regulators of MYC and EGR1 activity, respectively (Hurlin et al., 1999; Svaren et al., 1996). Transfac matrices representing the AP2 and ATF family of TFs (e.g., AP2alpha_01 and ATF1_Q6) were also uncovered in the F-match analysis. The Mediator kinase target KLF12 is a well-established repressor of AP2α activity (gene name: TFAP2A; Imhof et al., 1999), whereas the ATF2 and ATF7 proteins were each identified as Mediator kinase targets. Finally, enriched binding sites for E2F1 and SREBP, previously identified CDK8 kinase substrates (Morris et al., 2008; Zhao et al., 2012), were found by the F-match analysis shown in Figure 4D. Although these TFs were not identified in our HCT116 phosphoproteomics experiments, several co-regulators of E2F1 or SREBP activity (e.g., MGA and SIRT1; see Discussion) were among the high-confidence substrates listed in Table 1. Thus, there are many functional links between CA-dependent changes in gene expression (Figure 4A) and the Mediator kinase targets shown in Table 1.

Table 1. High-Confidence Mediator Kinase Substrates Identified Using CA and Quantitative Phosphoproteomics

Protein ID	Gene Name	Position	Location Probability	Ratio (H/L)	Adjusted p Value
Q9UHB7	AFF4	S31	0.79	0.209 ± 0.011	0.025
Q9UHB7	AFF4	S32	0.78	0.248 ± 0.070	0.056
Q9UHB7	AFF4	S1043	1.00	0.325 ± 0.035	0.020
Q9UHB7	AFF4	S814	1.00	0.410 ± 0.012	0.018
P15336	ATF2	S136	1.00	0.366 ± 0.012	0.015
P17544	ATF7	S434	0.88	0.302 ± 0.020	0.015
P17544	ATF7	S111	0.75	0.590 ± 0.062	0.082
P17544	ATF7	T112	0.99	0.593 ± 0.019	0.036
O00512	BCL9	S291	0.95	0.694 ± 0.031	0.092
Q12830	BPTF	S1300	1.00	0.691 ± 0.035	0.095
P38398	BRCA1	S1613	0.96	0.447 ± 0.036	0.025
Q9H8M2	BRD9	S588	1.00	0.455 ± 0.009	0.019
H0YBQ5;E5RFK5	CCNC;CCNC	S218;S272	1.00	0.642 ± 0.037	0.066
Q12873	CHD3	S1601	1.00	0.595 ± 0.036	0.048
Q14839	CHD4	T1553	0.94	0.096 ± 0.002	0.018
Q9P2D1	CHD7	T2153	0.99	0.572 ± 0.024	0.034
K4DI93	CUL4B	S15	0.90	0.394 ± 0.038	0.078
Q9UER7	DAXX	S671	1.00	0.651 ± 0.014	0.053
Q5T1V6	DDX59	S64/S76	0.99/0.76	0.535 ± 0.045	0.064
Q9NPF5	DMAP1	T409	1.00	0.134 ± 0.018	0.015
P19419	ELK1	S324	1.00	0.636 ± 0.058	0.092
Q52LR7	EPC2	T353	0.97	0.403 ± 0.019	0.059
Q96E09	FAM122A	S267	0.79	0.513 ± 0.082	0.085
Q12948	FOXC1	S241	1.00	0.433 ± 0.063	0.048
Q9NZM4	GLTSCR1	S755	1.00	0.394 ± 0.052	0.032
P15822	HIVEP1	S479	0.99	0.649 ± 0.019	0.055
Q7Z6Z7	HUWE1	S3816	0.98	0.527 ± 0.018	0.025
Q8NFU5	IPMK	S7	1.00	0.663 ± 0.050	0.098
Q9Y4C1	KDM3A	S445	1.00	0.448 ± 0.034	0.025
Q9Y4X4	KLF12	S202	1.00	0.441 ± 0.071	0.056
Q3ZCW2	LGALSL	S25	0.99	0.698 ± 0.029	0.092
Q92585	MAML1	S159	1.00	0.325 ± 0.009	0.015
Q92585	MAML1	S303	0.98	0.356 ± 0.018	0.049
Q14676	MDC1	S1775	1.00	0.453 ± 0.075	0.061
Q93074	MED12	S688	0.99	0.168 ± 0.036	0.020
Q9UHV7	MED13	S749	0.96	0.356 ± 0.041	0.073
Q71F56	MED13L	S878	1.00	0.568 ± 0.060	0.065
O60244	MED14	S1112	1.00	0.233 ± 0.045	0.025
O60244	MED14	S1128/S1136	0.99/0.99	0.100 ± 0.015	0.025
O95402	MED26	S314	1.00	0.177 ± 0.039	0.025
Q8IWI9	MGA	S2924	0.99	0.660 ± 0.032	0.070
O14686	MLL2	S3199	0.98	0.630 ± 0.019	0.047
P55197	MLLT10	S346	1.00	0.470 ± 0.005	0.076
O96007	MOCS2	S20	1.00	0.531 ± 0.035	0.034
Q9NV56	MRGBP	S195	1.00	0.611 ± 0.023	0.043
Q6P1R3	MSANTD2	S27	1.00	0.623 ± 0.053	0.085
Q2TAK8	MUM1	S326	1.00	0.582 ± 0.050	0.059
Q15742	NAB2	S162	1.00	0.573 ± 0.014	0.032

(Continued on next page)

Table 1. *Continued*

Protein ID	Gene Name	Position	Location Probability	Ratio (H/L)	Adjusted p Value
Q15788	NCOA1	S698	1.00	0.381 ± 0.042	0.081
Q9H3P2	NELFA	S363	0.96	0.403 ± 0.032	0.023
Q9H3P2	NELFA	S360	0.50	0.441 ± 0.039	0.092
Q6P4R8	NFRKB	S1291	1.00	0.688 ± 0.035	0.092
Q9NZT2	OGFR	S349	1.00	0.170 ± 0.015	0.025
Q9NZT2	OGFR	S484	0.99	0.348 ± 0.035	0.021
P29590	PML	S530	1.00	0.674 ± 0.012	0.059
Q6EEV4	POLR2M	S10	0.99	0.416 ± 0.018	0.019
Q5UIP0	RIF1	S1613	0.98	0.357 ± 0.014	0.048
Q5UIP0	RIF1	S1616	1.00	0.418 ± 0.051	0.033
Q92766	RREB1	S1653	1.00	0.237 ± 0.025	0.039
Q6SPF0	SAMD1	S425	0.94	0.418 ± 0.022	0.019
O15047	SETD1A	T1088	1.00	0.204 ± 0.010	0.015
Q7Z333	SETX	S2612	1.00	0.465 ± 0.018	0.080
Q96EB6	SIRT1	T530	1.00	0.201 ± 0.030	0.043
Q9UQ35	SRRM2	S2449	1.00	0.708 ± 0.004	0.081
P42224	STAT1	S727	0.99	0.367 ± 0.001	0.047
Q12962	TAF10	S44	1.00	0.565 ± 0.020	0.032
Q7Z2Z1	TICRR	S1413	0.99	0.472 ± 0.066	0.059
Q12888	TP53BP1	S265	1.00	0.258 ± 0.014	0.015
Q12888	TP53BP1	S525	1.00	0.600 ± 0.014	0.036
P13051	UNG	S63	0.84	0.473 ± 0.026	0.025
P13051	UNG	T60/S63	0.99/0.62	0.487 ± 0.027	0.025
Q9H0D6	XRN2	S487	1.00	0.566 ± 0.041	0.047
Q9NUA8	ZBTB40	T166	0.99	0.378 ± 0.078	0.058
A6NFI3	ZNF316	S10	1.00	0.598 ± 0.043	0.056
Q6ZN55	ZNF574	S717	1.00	0.406 ± 0.052	0.033
O15014	ZNF609	S804	1.00	0.373 ± 0.001	0.015

All sites correspond to reviewed accessions and canonical isoforms in Uniprot except for CCNC, whose identified site is not present in the canonical isoform. The "p value" column represents an adjusted p value from an empirical Bayes analysis (Ritchie et al., 2015). See also the Supplemental Information.

Cellular Proteome Changes Resulting from Mediator Kinase Inhibition

The ability of CDK8-dependent phosphorylation to regulate protein turnover has been reported in both yeast and human cells (Alarcón et al., 2009; Fryer et al., 2004; Nelson et al., 2003; Raithatha et al., 2012). We therefore hypothesized that CDK8/19 activity might modulate protein abundance for some of the substrates identified here. Rather than focus on selected Mediator kinase targets, we performed quantitative proteome analyses in CA-treated cells versus DMSO controls at six time points (t = 0 hr, 1 hr, 3 hr, 6 hr, 18 hr, and 24 hr). In this way, we were able to interrogate many cellular proteins at once and correlate changes in Mediator kinase activity with increased or decreased protein abundance. To complete these analyses, we used SILAC-labeled HCT116 cells, consistent with the phosphoproteomics experiments.

The analysis consisted of a CA treatment time course from 0 to 24 hr, with six time points being used in total to treat heavy (Arg10 and Lys8) or light (Arg0 and Lys0) HCT116 cell popula-

tions in biological replicate experiments (Figures 5A and 5B). Peptides were harvested in a manner similar to that used for phosphoproteomics, and 17 fractions from basic reversed-phase chromatography were analyzed for changes in H/L ratio at each time point. We found a high number of overlapping proteins across replicates, and CA treatment did not affect global H/L ratios for proteins across the time course in the replicates (Figure 5B). Given the ability of CDK8 to promote substrate turnover in response to specific biological phenomena (e.g., starvation; Nelson et al., 2003; Raithatha et al., 2012), we were somewhat surprised to find that CDK8/19 inhibition did not notably alter the abundance of the target proteins listed in Table 1, with the exception of MED13 and MED13L. A list of all quantified proteins in CA-treated versus untreated cells (0–24 hr) is provided in Table S4.

An empirical Bayes analysis of the data suggested that most proteome changes occurred at either 18 or 24 hr when compared to control (0 hr, in which both populations were DMSO treated), as shown by the volcano plot in Figure 5C.
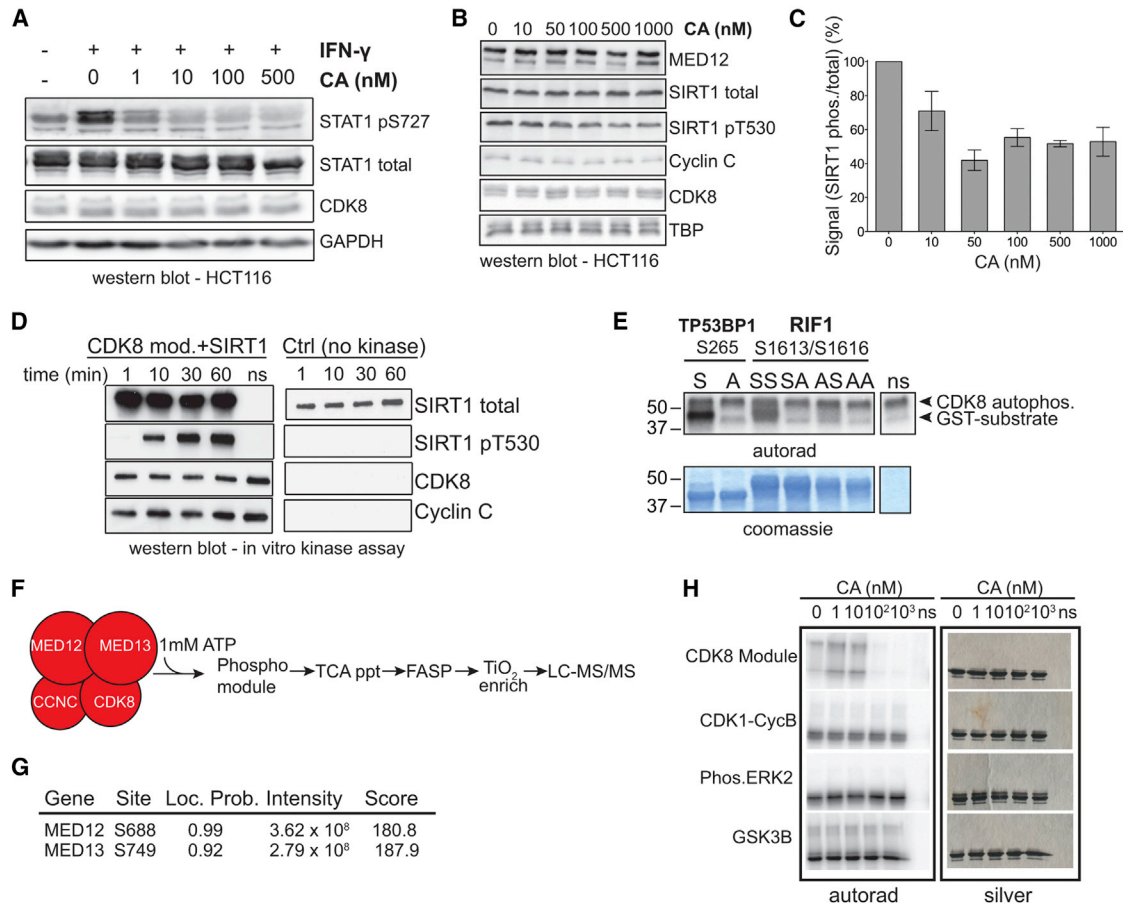
Figure 3. In Vitro Validation of Select CDK8/19 Substrates

(A) Validation of STAT1 S727 as a Mediator kinase target in HCT116 cells.

(B) Western blot validation of SIRT1 T530 as a Mediator kinase target. Levels of total SIRT1 and other proteins known to regulate CDK8 activity (MED12 or CCNC) remained unchanged. TBP is a loading control.

(C) Quantitation of data in (B). Error bars are SEM; n = 2 for technical replicates.

(D) In vitro kinase assay with recombinant CDK8 module and SIRT1. With increasing time, SIRT1 pT530 detection increases, indicating CDK8 is phosphorylating this site. Increase is not seen in no kinase or no substrate (ns) controls.

(E) In vitro kinase assay with GST-tagged TP53BP1 or RIF1 fragments. Alanine mutations at identified phosphorylation sites show reduced phosphorylation by CDK8.

(F) Overview of method for identifying MED12 and MED13 phosphorylation sites using recombinant CDK8 modules.

(G) Verification of MED12 S688 and MED13 S749 phosphorylation sites.

(H) In vitro kinase assay using CA and GST-pol II CTD as a substrate. Whereas each kinase tested phosphorylates this substrate, CA only inhibits the CDK8 module.

Approximately 200 proteins showed significant changes in abundance, and these are listed in Table S5 (adj. p value < 0.1). To further examine changes in the proteome with CA treatment, gene set enrichment analysis (GSEA) was employed (Subramanian et al., 2005). Using the hallmark gene set collection, we identified biological processes that displayed significant enrichment scores and false discovery rates (Figure 5D; Table S6). Of these signatures, several have been previously shown to be regulated by CDK8, including Wnt/β-catenin signaling, Notch signaling, hypoxia, interferon gamma response, and KRAS signaling (Bancerek et al., 2013; Firestein et al., 2008; Fryer et al., 2004; Galbraith et al., 2013; Morris et al., 2008; Xu et al., 2015). CDK8-dependent transcriptional changes have

been implicated in regulation of these pathways, and therefore, the proteome data corroborate these findings at the protein level. The GSEA results also reveal that proteome changes may selectively affect metabolic pathways in CA-treated HCT116 cells, with several (e.g., cholesterol homeostasis and fatty acid metabolism) previously linked to CDK8 kinase activity in model organisms (Zhao et al., 2012).

DISCUSSION

The natural product CA is an exceptionally selective inhibitor of the Mediator kinases CDK8 and CDK19 (Pelish et al., 2015). As such, it provided a means to rapidly and selectively probe
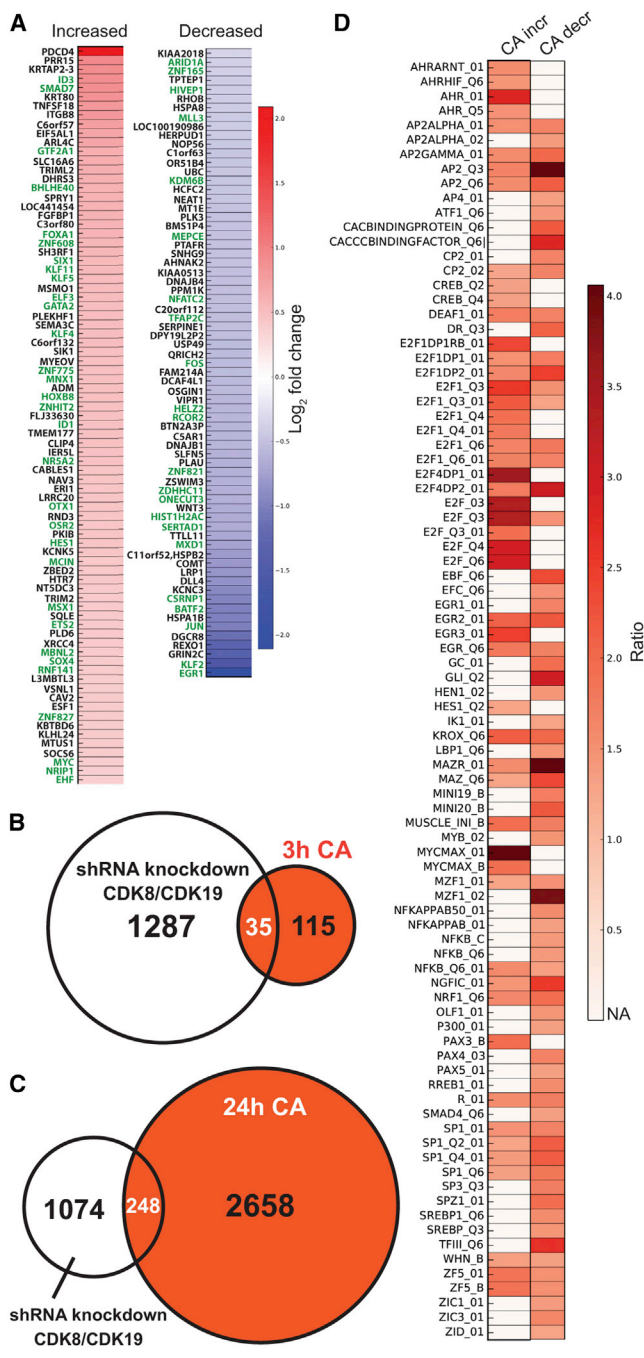
Figure 4. Mediator Kinase Inhibition Is Functionally Distinct from CDK8 or CDK19 Knockdown

(A) Heatmap of differentially expressed genes (RNA-seq) after 3 hr CA treatment. Green font represents transcription or chromatin regulator.

(B and C) Comparison with microarray data (Galbraith et al., 2013) using stable CDK8/19 knockdown (shRNA) versus 3 hr CA treatment (B) or 24 hr treatment (C) in HCT116 cells under normal growth conditions. A 1.5-fold cutoff was used for microarray data, and Cufflinks was used for CA-treated cells (no specific fold-change cutoff).

(D) TFBS analysis of promoters for genes whose expression changed with 3 hr CA treatment (listed in A). Promoters (±2 kb from the TSS of the canonical isoform) were analyzed using F-Match, part of the Transfac database. Over-

CDK8- and CDK19-dependent phosphoproteome changes in human cells. Because of their association with Mediator, CDK8 and CDK19 were expected to phosphorylate proteins involved in regulating pol II activity and chromatin architecture. In accordance with these expectations, our data support a primary role for Mediator kinases in pol II transcription and chromatin regulation. Strikingly, however, the direct impact of Mediator kinase inhibition on global pol II transcription was modest and affected a limited set of genes, at least under the conditions of this study. Limited transcriptional effects were also observed in CA-sensitive acute myeloid leukemia (AML) cell lines (Pelish et al., 2015).

At the gene expression level, it appears that Mediator kinases predominantly "regulate the regulators" of transcription. Many genes whose expression increased or decreased 1.5-fold or greater upon CA treatment are DNA-binding TFs or general transcription or chromatin regulators. Similarly, DNA-binding TFs and pol II transcription or chromatin regulators represented the majority of high-confidence CDK8/CDK19 kinase targets from the SILAC phosphoproteomics experiments. Quantitative proteomic data across a 24-hr time course implicated numerous signaling and metabolic pathways that appear to be regulated by Mediator kinase activity under normal growth conditions. Whereas these pathways can be linked to known transcriptional or phosphorylation targets of CDK8/CDK19 or those now identified here, much additional investigation will be required to delineate the molecular mechanisms by which Mediator kinases regulate specific signaling pathways or transcriptional processes.

CDK8/19 Phosphorylate Mediator Subunits and Post-initiation Transcription Regulators

CDK8 can reversibly associate with Mediator to form a CDK8-Mediator complex (Taatjes et al., 2002), and immunoprecipitation-mass spectrometry experiments in HeLa or HEK293T cells suggest CDK19 interacts similarly with Mediator (Daniels et al., 2013; Ebmeier and Taatjes, 2010; Sato et al., 2004). We identified eight high-confidence CDK8/19 phosphorylation sites in six different Mediator subunits: CCNC; MED12; MED13; MED13L; MED14; and MED26. CCNC, MED12, MED13, and MED13L each associate with CDK8 or CDK19 as part of the kinase module of Mediator. MED13 appears to be important for physical interaction between the kinase module and Mediator (Knuesel et al., 2009), and previous studies have shown that increased MED13 or MED13L abundance can increase the proportion of CDK8-Mediator versus core Mediator in cells (Davis et al., 2013). These previous results were shown in the context of inhibition of the E3 ubiquitin ligase FBW7, which ubiquitylates MED13 and MED13L to promote their degradation. Our quantitative whole-proteome data showed that the abundances of MED13 and MED13L were each increased in CA-treated HCT116 cells. FBW7-dependent ubiquitylation of MED13 or MED13L required prior modification at residue T326, a phospho-degron site in MED13 and MED13L (Davis et al., 2013). The CDK8/19 sites identified in MED13 and MED13L are distinct

represented sites with at least 1.5-fold increase versus control promoters are shown for Transfac vertebrate matrices. Matrix name is at left.

Figure 5. Quantitative Proteomics Reveals Pathways and Proteins Affected by Mediator Kinase Inhibition

(A) Overview of quantitative proteomics method.

(B) Venn diagram of biological replicates showing number of proteins identified in the time series. Replicates show a high degree of overlap for protein IDs.

(residue S749 and residue S878, respectively) and do not overlap with known or predicted phospho-degron motifs; thus, it remains unclear how Mediator kinase activity may affect MED13 or MED13L protein levels.

The MED26 subunit is generally absent from CDK8-Mediator purifications (Ebmeier and Taatjes, 2010; Sato et al., 2004; Taatjes et al., 2002), and hence, its phosphorylation by CDK8 or CDK19 may promote MED26 dissociation from Mediator. The CDK8/19 modification site on MED26 (S314), however, does not reside in regions required for Mediator association (Takahashi et al., 2011). The MED14 subunit is an important architectural factor within Mediator, and structural studies with reconstituted partial complexes and crosslinking-mass spectrometry (CXMS) revealed MED14 crosslinks with several Mediator subunits, including MED8 and MED7, involving MED14 residues 1,256 and 1,295, respectively (Cevher et al., 2014). These reside some distance (in sequence space) from the Mediator kinase phosphorylation sites (S1112, S1128, and S1136). Furthermore, CXMS and cryo-EM data with reconstituted yeast Mediator and yeast pol II revealed MED14 interactions with pol II and TFIIF (Plaschka et al., 2015). However, the *S. cerevisiae* Med14 subunit from this study consisted of residues 1–755 (of 1,082 residues in yeast Med14) and the human MED14 S1112, S1128, and S1136 residues do not appear to be conserved.

Knockdown experiments have implicated the CDK8 protein in the regulation of transcription elongation and/or pol II pausing or pause release (Donner et al., 2010; Galbraith et al., 2013). Furthermore, chromatin immunoprecipitation sequencing (ChIP-seq) data from CA-treated MOLM-14 cells indicated a reduced pol II travel ratio (TR) (ratio of promoter-bound pol II versus pol II in gene body) at genes whose expression was upregulated by CA (Pelish et al., 2015), implicating Mediator kinase activity in pol II pausing or pause release. The reduced TR in CA-treated cells could also reflect inhibition of premature pol II termination. Here, we identified AFF4, NELFA, MED26, POLR2M, SETX, and XRN2 as high-confidence Mediator kinase targets, and each of these factors has been implicated in regulation of pol II pausing, premature termination, or elongation (Brannan et al., 2012; Cheng et al., 2012; Jishage et al., 2012; Kwak and Lis, 2013; Lin et al., 2010; Takahashi et al., 2011; Wagschal et al., 2012).

Mediator Kinases as Potential Metabolic Regulators

CDK8 orthologs in *Drosophila* and yeast have been linked to lipid and glucose metabolism and regulation of cellular responses to nutrient stress (Kuchin et al., 1995; Lindsay et al., 2014; Mousley et al., 2012; Zhao et al., 2012). Upon Mediator kinase inhibition by CA, we observed changes in the abundance of about 200 proteins (Figure 5), including many involved in basic metabolic pathways such as oxidative phosphorylation, fatty acid metabolism,

and cholesterol homeostasis. MED13 and CCNC appear to regulate mitochondrial function in yeast (Cooper et al., 2014; Khakhina et al., 2014), and overexpression of MED13 in mouse cardiac tissue alters fatty acid metabolism, β-oxidation, and mitochondrial content (Baskin et al., 2014). We identified MED13 and CCNC as Mediator kinase substrates and observed an increase in MED13 protein levels upon CA treatment, which could contribute to altered fatty acid metabolism or oxidative phosphorylation observed in CA-treated cells (Figure 5D).

CDK8 kinase activity has previously been linked to cholesterol metabolism and fatty acid synthesis via regulation of SREBP. In particular, CDK8-dependent phosphorylation of SREBP residue T402 correlated with SREBP degradation in *Drosophila* and mouse cells (Zhao et al., 2012). GSEA analysis of whole-proteome data identified changes in the cholesterol homeostasis, adipogenesis, and fatty acid metabolism hallmark signatures in CA-treated cells (Figure 5D). Moreover, F-match identified SREBP-binding motifs as over-represented among genes whose expression changed upon CA treatment (Figure 4D). Whereas phosphorylation of SREBP T402 was detected in our phosphoproteomics experiments, its level was not altered in CA-treated cells, suggesting alternate means of Mediator kinase-dependent SREBP regulation in HCT116 cells. Other kinases, including GSK3β (Sundqvist et al., 2005), are known to target SREBP T402, and we have confirmed that CA does not inhibit GSK3β in cell lysates (Pelish et al., 2015) or in in vitro kinase assays with the purified protein (Figure 3H). Therefore, the SREBP T402 phosphorylation level may remain constant in CA-treated cells due to other kinases targeting this site. Alternately, SREBP may not be a substrate for CDK8 in HCT116 cells. SIRT1, a validated Mediator kinase target, can negatively regulate SREBP activity through deacetylation (Walker et al., 2010). The Mediator kinases phosphorylate SIRT1 at residue T530, and phosphorylation at T530 has been shown to activate the SIRT1 deacetylase (Sasaki et al., 2008). Thus, via SIRT1 and potentially other substrates, Mediator kinases may regulate cholesterol or fatty acid metabolism independent of direct SREBP phosphorylation in HCT116 cells.

Human Mediator Kinases and TF Turnover

Previous studies revealed that phosphorylation of nutrient-responsive TFs Gcn4, Ste12, or Phd1 by yeast Cdk8 promoted their degradation (Chi et al., 2001; Nelson et al., 2003; Raithatha et al., 2012). Studies in metazoans have shown evidence for CDK8-dependent phosphorylation of the TFs SMAD1, SMAD3, Notch ICD, SREBP, E2F1, and STAT1 (Alarcón et al., 2009; Bancerek et al., 2013; Fryer et al., 2004; Morris et al., 2008; Zhao et al., 2012). Among these, increased degradation of the Notch ICD, SMAD1, SMAD3, and SREBP correlated with phosphorylation. For these reasons, we anticipated that inhibition of CDK8 and

---

(C) Volcano plot comparing protein abundance at 18 hr and 24 hr time points versus control (0 hr). Adjusted p values are colored according to an empirical Bayes analysis.

(D) Individual analysis of t = 3 hr, 6 hr, 18 hr, and 24 hr CA treatment time points using GSEA and the hallmark gene sets from the Molecular Signatures Database. Comparison of the t = 0 hr and 1 hr time points showed no differences in the hallmark gene sets (not shown). The color of the heatmap corresponds to the direction and magnitude of the normalized enrichment score for that gene set at each time point, compared to t = 0 hr controls. "NA" and the corresponding color indicate a hallmark gene set not being identified from the proteome data at the designated time.

(E) Protein abundance increases for MED13 and MED13L in CA-treated cells.

CDK19 kinase activity would affect the protein levels of a subset of their targets. Whole-proteome data revealed no evidence that TF phosphorylation by Mediator kinases affected their stability, even with analyses at 1, 3, 6, 18, or 24 hr of CA treatment. In fact, we found little evidence for altered stability of any high-confidence Mediator kinase targets, with the notable exception of MED13 and MED13L. Despite this result, cell type or context may be key factors that dictate the effect of Mediator kinase phosphorylation on protein turnover. Here, we evaluated HCT116 cells in normal growth conditions whereas Mediator kinases may in fact more generally regulate substrate protein turnover during stress responses or at different developmental stages.

Whereas no changes in TF turnover were evident from the whole-proteome data in CA-treated versus control cells, we identified many links between the gene expression changes and the phosphoproteomics data (Figure S4). These results are consistent with Mediator kinases affecting TF activity in HCT116 cells under normal growth conditions, rather than TF turnover.

CDK8 as a Colon Cancer Oncogene: Mediator Kinase Inhibition versus Subunit Knockdown

CDK8 was identified as a colon cancer oncogene in part through a shRNA screen for genes required for HCT116 cell proliferation (Firestein et al., 2008). CDK8 was one of 166 candidates in this screen; CDK8 was also identified in a screen for factors required for activation of a β-catenin-driven reporter in a different colon cancer line, DLD-1 (Firestein et al., 2008). Our analyses with CA indicate that, in contrast to CDK8 knockdown, Mediator kinase inhibition does not affect HCT116 cell growth (Pelish et al., 2015). These findings highlight the distinction between physical loss of a protein versus targeted inhibition of its enzymatic activity.

As a TF, β-catenin assembles with the DNA-binding proteins TCF and LEF-1 to activate genes that drive cell proliferation. HCT116 cells are heterozygous for a mutant β-catenin protein that is resistant to degradation (Morin et al., 1997). Consequently, HCT116 cells have increased β-catenin levels and are considered "β-catenin dependent." Consistent with an oncogenic function for CDK8, CDK8 knockdown prevented activation of β-catenin target genes in colon cancer cell lines (Firestein et al., 2008). In addition, the E2F1 TF has been shown to be an important negative regulator of β-catenin stability (through unknown mechanisms), and elevated levels of the CDK8 protein, as observed in HCT116 cells (Firestein et al., 2008), can block E2F1-dependent inhibition of β-catenin target gene expression (Morris et al., 2008). Thus, in colon cancer cells, the CDK8 protein appears to upregulate β-catenin target gene expression in two ways: as a β-catenin co-activator and as an inhibitor of E2F1 activity.

Whereas E2F1 and β-catenin activity or stability is known to be regulated by phosphorylation, we did not observe significant changes in E2F1 or β-catenin protein or phosphopeptide levels in CA-treated HCT116 cells. An F-match analysis based upon gene expression changes in CA-treated cells, however, identified E2F binding motifs as over-represented (Figure 4D), and Ingenuity Pathway Analysis (IPA) of upstream regulators identified

β-catenin target genes as over-represented among those whose expression increased or decreased upon CA treatment (Table S7). GSEA of our proteomics data (CA-treated versus untreated; 0–24 hr) revealed upregulation of the E2F1 and β-catenin pathways (Figure 5D). Furthermore, numerous high-confidence Mediator kinase substrates are known to directly regulate β-catenin or E2F activity, and these are summarized in Table S8.

Although these results implicate Mediator kinase activity in the regulation of E2F1 and β-catenin transcription networks in HCT116 cells, the effects of Mediator kinase inhibition are clearly distinct from CDK8 or CDK19 knockdown (Donner et al., 2010; Firestein et al., 2008; Galbraith et al., 2013). This was not unexpected, as the physical presence of an enzyme typically serves structural roles, such as maintaining the integrity of a multi-protein complex. For example, ablation of the CDK7 ortholog in yeast (Kin28) abolishes essentially all pol II transcription (Holstege et al., 1998), in contrast to targeted inhibition of Kin28 activity (Kanin et al., 2007). Direct comparison of the transcriptional changes that resulted from physical loss of the CDK8 or CDK19 protein versus targeted inhibition of kinase activity (i.e., with protein levels remaining intact) revealed stark differences in the genes affected and the magnitude of gene expression changes. These differences highlight the importance of a structural or "scaffolding" role of the CDK8 or CDK19 proteins. Indeed, CDK8 knockdown decreases MED12 levels and increases CDK19 protein levels in HCT116 cells (Donner et al., 2010; Galbraith et al., 2013), which likely contributes to the distinct gene expression and anti-proliferative effects of CDK8 knockdown (Firestein et al., 2008) compared with kinase inhibition by CA. Because CA inhibits CDK19 as well as CDK8 (Pelish et al., 2015), this may also result in compensatory effects that distinguish the CDK8 knockdown phenotype from CDK8/CDK19 inhibition. Future studies are needed to more precisely establish the roles of CDK8 versus CDK19 in regulating the elaborate E2F1, β-catenin, and other inter-related signaling networks that contribute to HCT116 survival and proliferation.

Conclusions

This study provides a large-scale identification of Mediator kinase substrates and the impact of Mediator kinase activity on pol II transcription and the cellular proteome. In comparison with the ~170 potential CDK9 kinase substrates recently identified in HCT116 cells (Sansó et al., 2016), it is notable that the high-confidence substrates for CDK9 are distinct from the Mediator kinases. This further suggests that CDK9 (e.g., as part of P-TEFb or the SEC) and Mediator kinases play non-redundant roles in transcription regulation.

Our results were enabled by the rigorous biochemical, cellular, and biophysical characterization of CA, which demonstrated that it represents an unusual case of an inhibitor that is truly selective for Mediator kinases in human cells (Pelish et al., 2015). The data and methodologies presented provide a valuable resource for further delineation of the molecular mechanisms whereby Mediator kinases, and their substrates, regulate processes that are fundamentally important in human development and disease. For example, the methodologies described could be applied toward other cell types or contexts to uncover cell-type- or context-specific roles for Mediator kinases. Alternately,

the Mediator kinase targets or proteome changes identified here could be further tested for their mechanistic role(s) in regulating chromatin structure and function, DNA repair or replication, cell metabolism, or pol II transcription.

EXPERIMENTAL PROCEDURES

Cell Culture

HCT116 cells were cultured in DMEM supplemented with 10% fetal bovine serum (FBS) and penicillin/streptomycin. Cells were maintained at 37°C and 5% CO_2.

SILAC Labeling

HCT116 cells were cultured in DMEM lacking arginine and lysine (Pierce, 88420) supplemented with either Arg10 (33.6 μg/ml) and Lys8 (73 μg/ml) or Arg0 and Lys0 for heavy and light treatment, respectively. After six passages at 1:3 ratio, cells were tested for Arg/Lys incorporation and were subsequently supplemented with 200 mg/l of proline (Sigma-Aldrich, P5607) as a small amount of Arg→Pro conversion was detected. Cells were maintained in 10% dialyzed FBS and penicillin/streptomycin.

TiO₂ Phosphopeptide Enrichment, ERLIC Chromatography, and LC-MS/MS

Protocols were carried out as described (Stuart et al., 2015). An Orbitrap LTQ (Thermo Fisher) was used for phosphoproteomics, and an Orbitrap Velos (Thermo Fisher) was used for quantitative proteome analysis.

In Vitro Kinase Assays

Assays were done essentially as described (Bancerek et al., 2013). Additional details are provided in Supplemental Experimental Procedures.

Gene Expression Comparison between CA-Treated HCT116 Cells and shRNA CDK8/19

shRNA CDK8 and CDK19 microarray data were obtained from the GEO (accession number: GSE38061), and data under the "normoxia" tab were used for the comparison to CA-treated cells.

ACCESSION NUMBERS

The accession numbers for the RNA-seq data reported in this paper are GEO: GSE65161 and GEO: GSE78506. The accession number for the proteomics data reported in this paper is ProteomeXchange PRIDE: PXD003698.

SUPPLEMENTAL INFORMATION

Supplemental Information includes Supplemental Experimental Procedures, four figures, and eight tables and can be found with this article online at http://dx.doi.org/10.1016/j.celrep.2016.03.030.

AUTHOR CONTRIBUTIONS

C.C.E., Z.C.P., and W.M.O. performed MS sample prep and analysis. A.T.O. and R.D.D. analyzed RNA-seq data. T.L. assisted with proteome data analysis. A.T., H.E.P., and M.D.S. provided key reagents and advice. Z.C.P. and D.J.T. designed and performed experiments, analyzed data, and wrote the manuscript.

ACKNOWLEDGMENTS

REFERENCES

Alarcón, C., Zaromytidou, A.I., Xi, Q., Gao, S., Yu, J., Fujisawa, S., Barlas, A., Miller, A.N., Manova-Todorova, K., Macias, M.J., et al. (2009). Nuclear CDKs drive Smad transcriptional activation and turnover in BMP and TGF-beta pathways. Cell 139, 757–769.

Allen, B.L., and Taatjes, D.J. (2015). The Mediator complex: a central integrator of transcription. Nat. Rev. Mol. Cell Biol. 16, 155–166.

Bancerek, J., Poss, Z.C., Steinparzer, I., Sedlyarov, V., Pfaffenwimmer, T., Mikulic, I., Dölken, L., Strobl, B., Müller, M., Taatjes, D.J., and Kovarik, P. (2013). CDK8 kinase phosphorylates transcription factor STAT1 to selectively regulate the interferon response. Immunity 38, 250–262.

Baskin, K.K., Grueter, C.E., Kusminski, C.M., Holland, W.L., Bookout, A.L., Satapati, S., Kong, Y.M., Burgess, S.C., Malloy, C.R., Scherer, P.E., et al. (2014). MED13-dependent signaling from the heart confers leanness by enhancing metabolism in adipose tissue and liver. EMBO Mol. Med. 6, 1610–1621.

Brannan, K., Kim, H., Erickson, B., Glover-Cutter, K., Kim, S., Fong, N., Kiemele, L., Hansen, K., Davis, R., Lykke-Andersen, J., and Bentley, D.L. (2012). mRNA decapping factors and the exonuclease Xrn2 function in widespread premature termination of RNA polymerase II transcription. Mol. Cell 46, 311–324.

Cevher, M.A., Shi, Y., Li, D., Chait, B.T., Malik, S., and Roeder, R.G. (2014). Reconstitution of active human core Mediator complex reveals a critical role of the MED14 subunit. Nat. Struct. Mol. Biol. 21, 1028–1034.

Cheng, B., Li, T., Rahl, P.B., Adamson, T.E., Loudas, N.B., Guo, J., Varzavand, K., Cooper, J.J., Hu, X., Gnatt, A., et al. (2012). Functional association of Gdown1 with RNA polymerase II poised on human genes. Mol. Cell 45, 38–50.

Chi, Y., Huddleston, M.J., Zhang, X., Young, R.A., Annan, R.S., Carr, S.A., and Deshaies, R.J. (2001). Negative regulation of Gcn4 and Msn2 transcription factors by Srb10 cyclin-dependent kinase. Genes Dev. 15, 1078–1092.

Colaert, N., Helsens, K., Martens, L., Vandekerckhove, J., and Gevaert, K. (2009). Improved visualization of protein consensus sequences by iceLogo. Nat. Methods 6, 786–787.

Cooper, K.F., Khakhina, S., Kim, S.K., and Strich, R. (2014). Stress-induced nuclear-to-cytoplasmic translocation of cyclin C promotes mitochondrial fission in yeast. Dev. Cell 28, 161–173.

Daniels, D.L., Ford, M., Schwinn, M.K., Benink, H., Galbraith, M.D., Amunugama, R., Jones, R., Allen, D., Okazaki, N., Yamakawa, H., et al. (2013). Mutual exclusivity of MED12/MED12L, MED13/13L, and CDK8/19 paralogs revealed within the CDK-Mediator kinase module. J. Proteomics Bioinform. S2, 004.

Davis, M.A., Larimore, E.A., Fissel, B.M., Swanger, J., Taatjes, D.J., and Clurman, B.E. (2013). The SCF-Fbw7 ubiquitin ligase degrades MED13 and MED13L and regulates CDK8 module association with Mediator. Genes Dev. 27, 151–156.

Donner, A.J., Ebmeier, C.C., Taatjes, D.J., and Espinosa, J.M. (2010). CDK8 is a positive regulator of transcriptional elongation within the serum response network. Nat. Struct. Mol. Biol. 17, 194–201.

Ebmeier, C.C., and Taatjes, D.J. (2010). Activator-Mediator binding regulates Mediator-cofactor interactions. Proc. Natl. Acad. Sci. USA 107, 11283–11288.

Firestein, R., Bass, A.J., Kim, S.Y., Dunn, I.F., Silver, S.J., Guney, I., Freed, E., Ligon, A.H., Vena, N., Ogino, S., et al. (2008). CDK8 is a colorectal cancer oncogene that regulates beta-catenin activity. Nature 455, 547–551.

Fryer, C.J., White, J.B., and Jones, K.A. (2004). Mastermind recruits CycC:CDK8 to phosphorylate the Notch ICD and coordinate activation with turnover. Mol. Cell 16, 509–520.

Galbraith, M.D., Allen, M.A., Bensard, C.L., Wang, X., Schwinn, M.K., Qin, B., Long, H.W., Daniels, D.L., Hahn, W.C., Dowell, R.D., and Espinosa, J.M. (2013). HIF1A employs CDK8-mediator to stimulate RNAPII elongation in response to hypoxia. Cell 153, 1327–1339.

Holstege, F.C., Jennings, E.G., Wyrick, J.J., Lee, T.I., Hengartner, C.J., Green, M.R., Golub, T.R., Lander, E.S., and Young, R.A. (1998). Dissecting the regulatory circuitry of a eukaryotic genome. Cell 95, 717–728.

Hurlin, P.J., Steingrìmsson, E., Copeland, N.G., Jenkins, N.A., and Eisenman, R.N. (1999). Mga, a dual-specificity transcription factor that interacts with Max and contains a T-domain DNA-binding motif. EMBO J. 18, 7019–7028.

Imhof, A., Schuierer, M., Werner, O., Moser, M., Roth, C., Bauer, R., and Buettner, R. (1999). Transcriptional regulation of the AP-2alpha promoter by BTEB-1 and AP-2rep, a novel wt-1/egr-related zinc finger repressor. Mol. Cell. Biol. 19, 194–204.

Jishage, M., Malik, S., Wagner, U., Uberheide, B., Ishihama, Y., Hu, X., Chait, B.T., Gnatt, A., Ren, B., and Roeder, R.G. (2012). Transcriptional regulation by Pol II(G) involving mediator and competitive interactions of Gdown1 and TFIIF with Pol II. Mol. Cell 45, 51–63.

Kagey, M.H., Newman, J.J., Bilodeau, S., Zhan, Y., Orlando, D.A., van Berkum, N.L., Ebmeier, C.C., Goossens, J., Rahl, P.B., Levine, S.S., et al. (2010). Mediator and cohesin connect gene expression and chromatin architecture. Nature 467, 430–435.

Kanin, E.I., Kipp, R.T., Kung, C., Slattery, M., Viale, A., Hahn, S., Shokat, K.M., and Ansari, A.Z. (2007). Chemical inhibition of the TFIIH-associated kinase Cdk7/Kin28 does not impair global mRNA synthesis. Proc. Natl. Acad. Sci. USA 104, 5812–5817.

Khakhina, S., Cooper, K.F., and Strich, R. (2014). Med13p prevents mitochondrial fission and programmed cell death in yeast through nuclear retention of cyclin C. Mol. Biol. Cell 25, 2807–2816.

Knuesel, M.T., Meyer, K.D., Bernecky, C., and Taatjes, D.J. (2009). The human CDK8 subcomplex is a molecular switch that controls Mediator coactivator function. Genes Dev. 23, 439–451.

Kuchin, S., Yeghiayan, P., and Carlson, M. (1995). Cyclin-dependent protein kinase and cyclin homologs SSN3 and SSN8 contribute to transcriptional control in yeast. Proc. Natl. Acad. Sci. USA 92, 4006–4010.

Kwak, H., and Lis, J.T. (2013). Control of transcriptional elongation. Annu. Rev. Genet. 47, 483–508.

Lin, C., Smith, E.R., Takahashi, H., Lai, K.C., Martin-Brown, S., Florens, L., Washburn, M.P., Conaway, J.W., Conaway, R.C., and Shilatifard, A. (2010). AFF4, a component of the ELL/P-TEFb elongation complex and a shared subunit of MLL chimeras, can link transcription elongation to leukemia. Mol. Cell 37, 429–437.

Lindsay, A.K., Morales, D.K., Liu, Z., Grahl, N., Zhang, A., Willger, S.D., Myers, L.C., and Hogan, D.A. (2014). Analysis of Candida albicans mutants defective in the Cdk8 module of mediator reveal links between metabolism and biofilm formation. PLoS Genet. 10, e1004567.

Liu, Y., Kung, C., Fishburn, J., Ansari, A.Z., Shokat, K.M., and Hahn, S. (2004). Two cyclin-dependent kinases promote RNA polymerase II transcription and formation of the scaffold complex. Mol. Cell. Biol. 24, 1721–1735.

Luo, Z., Lin, C., and Shilatifard, A. (2012). The super elongation complex (SEC) family in transcriptional control. Nat. Rev. Mol. Cell Biol. 13, 543–547.

Margolin, A.A., Ong, S.E., Schenone, M., Gould, R., Schreiber, S.L., Carr, S.A., and Golub, T.R. (2009). Empirical Bayes analysis of quantitative proteomics experiments. PLoS ONE 4, e7454.

Morin, P.J., Sparks, A.B., Korinek, V., Barker, N., Clevers, H., Vogelstein, B., and Kinzler, K.W. (1997). Activation of beta-catenin-Tcf signaling in colon cancer by mutations in beta-catenin or APC. Science 275, 1787–1790.

Morris, E.J., Ji, J.Y., Yang, F., Di Stefano, L., Herr, A., Moon, N.S., Kwon, E.J., Haigis, K.M., Näär, A.M., and Dyson, N.J. (2008). E2F1 represses beta-catenin transcription and is antagonized by both pRB and CDK8. Nature 455, 552–556.

Mousley, C.J., Yuan, P., Gaur, N.A., Trettin, K.D., Nile, A.H., Deminoff, S.J., Dewar, B.J., Wolpert, M., Macdonald, J.M., Herman, P.K., et al. (2012). A ste-

rol-binding protein integrates endosomal lipid metabolism with TOR signaling and nitrogen sensing. Cell 148, 702–715.

Nelson, C., Goto, S., Lund, K., Hung, W., and Sadowski, I. (2003). Srb10/Cdk8 regulates yeast filamentous growth by phosphorylating the transcription factor Ste12. Nature 421, 187–190.

Pelish, H.E., Liau, B.B., Nitulescu, I.I., Tangpeerachaikul, A., Poss, Z.C., Da Silva, D.H., Caruso, B.T., Arefolov, A., Fadeyi, O., Christie, A.L., et al. (2015). Mediator kinase inhibition further activates super-enhancer-associated genes in AML. Nature 526, 273–276.

Plaschka, C., Larivière, L., Wenzeck, L., Seizl, M., Hemann, M., Tegunov, D., Petrotchenko, E.V., Borchers, C.H., Baumeister, W., Herzog, F., et al. (2015). Architecture of the RNA polymerase II-Mediator core initiation complex. Nature 518, 376–380.

Raithatha, S., Su, T.C., Lourenco, P., Goto, S., and Sadowski, I. (2012). Cdk8 regulates stability of the transcription factor Phd1 to control pseudohyphal differentiation of Saccharomyces cerevisiae. Mol. Cell. Biol. 32, 664–674.

Ritchie, M.E., Phipson, B., Wu, D., Hu, Y., Law, C.W., Shi, W., and Smyth, G.K. (2015). limma powers differential expression analyses for RNA-sequencing and microarray studies. Nucleic Acids Res. 43, e47.

Sansó, M., Levin, R.S., Lipp, J.J., Wang, V.Y., Greifenberg, A.K., Quezada, E.M., Ali, A., Ghosh, A., Larochelle, S., Rana, T.M., et al. (2016). P-TEFb regulation of transcription termination factor Xrn2 revealed by a chemical genetic screen for Cdk9 substrates. Genes Dev. 30, 117–131.

Sasaki, T., Maier, B., Koclega, K.D., Chruszcz, M., Gluba, W., Stukenberg, P.T., Minor, W., and Scrable, H. (2008). Phosphorylation regulates SIRT1 function. PLoS ONE 3, e4020.

Sato, S., Tomomori-Sato, C., Parmely, T.J., Florens, L., Zybailov, B., Swanson, S.K., Banks, C.A.S., Jin, J., Cai, Y., Washburn, M.P., et al. (2004). A set of consensus mammalian mediator subunits identified by multidimensional protein identification technology. Mol. Cell 14, 685–691.

Stuart, S.A., Houel, S., Lee, T., Wang, N., Old, W.M., and Ahn, N.G. (2015). A phosphoproteomic comparison of B-RAFV600E and MKK1/2 inhibitors in melanoma cells. Mol. Cell. Proteomics 14, 1599–1615.

Subramanian, A., Tamayo, P., Mootha, V.K., Mukherjee, S., Ebert, B.L., Gillette, M.A., Paulovich, A., Pomeroy, S.L., Golub, T.R., Lander, E.S., and Mesirov, J.P. (2005). Gene set enrichment analysis: a knowledge-based approach for interpreting genome-wide expression profiles. Proc. Natl. Acad. Sci. USA 102, 15545–15550.

Sundqvist, A., Bengoechea-Alonso, M.T., Ye, X., Lukiyanchuk, V., Jin, J., Harper, J.W., and Ericsson, J. (2005). Control of lipid metabolism by phosphorylation-dependent degradation of the SREBP family of transcription factors by SCF(Fbw7). Cell Metab. 1, 379–391.

Svaren, J., Sevetson, B.R., Apel, E.D., Zimonjic, D.B., Popescu, N.C., and Milbrandt, J. (1996). NAB2, a corepressor of NGFI-A (Egr-1) and Krox20, is induced by proliferative and differentiative stimuli. Mol. Cell. Biol. 16, 3545–3553.

Szklarczyk, D., Franceschini, A., Wyder, S., Forslund, K., Heller, D., Huerta-Cepas, J., Simonovic, M., Roth, A., Santos, A., Tsafou, K.P., et al. (2015). STRING v10: protein-protein interaction networks, integrated over the tree of life. Nucleic Acids Res. 43, D447–D452.

Taatjes, D.J., Näär, A.M., Andel, F., 3rd, Nogales, E., and Tjian, R. (2002). Structure, function, and activator-induced conformations of the CRSP coactivator. Science 295, 1058–1062.

Takahashi, H., Parmely, T.J., Sato, S., Tomomori-Sato, C., Banks, C.A., Kong, S.E., Szutorisz, H., Swanson, S.K., Martin-Brown, S., Washburn, M.P., et al. (2011). Human mediator subunit MED26 functions as a docking site for transcription elongation factors. Cell 146, 92–104.

Ubersax, J.A., and Ferrell, J.E., Jr. (2007). Mechanisms of specificity in protein phosphorylation. Nat. Rev. Mol. Cell Biol. 8, 530–541.

Wagschal, A., Rousset, E., Basavarajaiah, P., Contreras, X., Harwig, A., Laurent-Chabalier, S., Nakamura, M., Chen, X., Zhang, K., Meziane, O., et al. (2012). Microprocessor, Setx, Xrn2, and Rrp6 co-operate to induce premature termination of transcription by RNAPII. Cell 150, 1147–1157.

Walker, A.K., Yang, F., Jiang, K., Ji, J.Y., Watts, J.L., Purushotham, A., Boss, O., Hirsch, M.L., Ribich, S., Smith, J.J., et al. (2010). Conserved role of SIRT1 orthologs in fasting-dependent inhibition of the lipid/cholesterol regulator SREBP. Genes Dev. *24*, 1403–1417.

Xu, W., Wang, Z., Zhang, W., Qian, K., Li, H., Kong, D., Li, Y., and Tang, Y. (2015). Mutated K-ras activates CDK8 to stimulate the epithelial-to-mesen-

chymal transition in pancreatic cancer in part via the Wnt/β-catenin signaling pathway. Cancer Lett. *356* (*2 Pt B*), 613–627.

Zhao, X., Feng, D., Wang, Q., Abdulla, A., Xie, X.J., Zhou, J., Sun, Y., Yang, E.S., Liu, L.P., Vaitheesvaran, B., et al. (2012). Regulation of lipogenesis by cyclin-dependent kinase 8-mediated control of SREBP-1. J. Clin. Invest. *122*, 2417–2427.